Development of Au Nano-particles Cladding-doped Optical Fiber for Surface Plasmon Resonance Sensor Applications

Seongmin Ju, Seongmook Jeong, Youngwoong Kim, Poram Jeon, and Won-Taek Han
School of Information and Communications/Department of Photonics and Applied Physics, Gwangju Institute of Science and Technology, Gwangju, South Korea
e-mail: jusm@gist.ac.kr, seongmook@gist.ac.kr, kyw@gist.ac.kr, porams@gist.ac.kr, wthan@gist.ac.kr

Seongjae Boo
Solar Center, Korea Institute of Industrial Technology, Gwangju, South Korea
e-mail: sboo@kitech.re.kr

Pramod R. Watekar
Sterlite Optical Technologies, E1, E2, E3, MIDC, Waluj, Aurangabad, India
e-mail: pramod.watekar@sterlite.com

***Abstract* — A novel optical fiber having its cladding doped with Au nano-particles was developed by modified chemical vapor deposition process. Absorption peaks of the optical fiber preform and the fiber appearing at 585 nm and 428 nm, respectively were due to surface plasmon resonance (SPR) of the incorporated Au nano-particles in the cladding. The measured peak wavelength of the SPR was found to increase from 480.9 nm to 505.5 nm with refractive index (n) from 1.406 to 1.436 and the SPR sensitivity was estimated to be 820 nm/RIU.**

Keywords - nano-particles; cladding-doped optical fiber; absorption; surface plasmon resonance.

I. INTRODUCTION

Recently, optical fiber sensors based on surface plasmon resonance (SPR) have gained attraction of scientists and engineers due to their all-optical remote sensing capability to measure various chemical, physical, and biological quantities [1-11]. SPR sensing phenomenon of the optical fiber can be divided into two categories, a propagating SPR and a localized SPR. The former can be obtained from thin metal coating onto the surface of optical fiber and a surface plasmon comes from extended charge waves traveling on the interface of metal and glass that are excited when dispersion of output light matches with that of incident light. Therefore, it is evanescent electromagnetic waves bounded by metal-glass interfaces induced by oscillations of the conduction electrons in the metal [12-14]. The latter is usually observed by confined colloidal, periodic, nano-systems [6][14-25], and a localized surface plasmon gets resonantly excited when the wavelength of incident light is equal to the characteristic wavelength of metal nano-particles [11-14]. It comes from confined conduction electrons oscillating in resonance with the electromagnetic field. In general, the excitation of surface plasmon is known to occur when the wave vector of the propagation constant of evanescent wave exactly matches with that of the surface plasmon of similar frequency and state of polarization. This occurs at a particular angle of incidence and the corresponding resonance condition for surface plasmons. The sharp absorption peak is observed at resonance angle because of reduction in the energy of the reflected light due to its energy transfer to surface plasmons. The resonance angle is very sensitive to variation in the refractive index of the sensing layer [1-5][8-11].

Optical fiber sensors based on SPR usually use thin metal film or nano-particles of Au or Ag because these noble metals present a sharp and intense plasmonic band in their internal reflectance spectrum when excited in the Kretschmann configuration of SPR [1-5][12-14]. To increase the sensitivity of optical fiber based SPR sensor, various configurations of optical fiber such as polished fiber, tapered fiber, grated fiber and coated fiber have been suggested [1-8][10-12][16]. Also, to improve the SPR sensing performance, effect of size, thickness, shape, and composition of plasmonic materials have been studied [4-6][25-28]. Despite all the efforts, however, optical fiber SPR sensors with controlled coating parameters have limitations: handling difficulty, difficulty of mass production, and high manufacturing cost.

In this paper, we developed a novel optical fiber incorporated with Au nano-particles (NPs) in cladding region, which is the first in the world to the best of our knowledge, allowing simple fabrication process due to no metal coating needed, mass production and compatibility with the existing SPR probe. Optical fiber sensor based on SPR of the fabricated fiber was demonstrated and in particular effect of environmental refractive index change on the SPR characteristics was investigated.

II. EXPERIMENTAL

The optical fiber incorporated with Au NPs in cladding region was fabricated by using the modified chemical vapor deposition (MCVD) and the fiber drawing processes. The

 ISBN: 978-1-61208-208-0

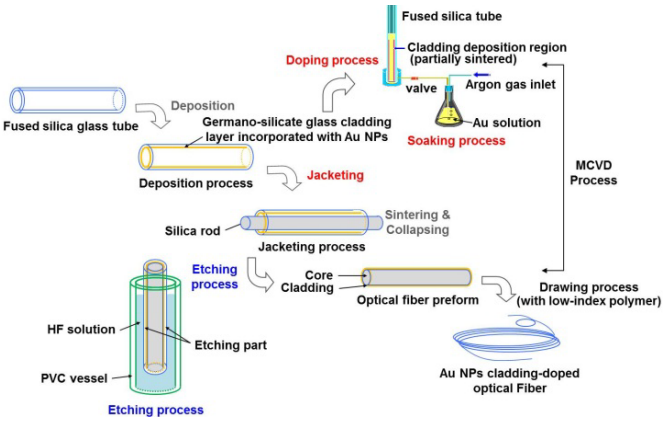

Figure 1. Schematic flow diagram of the fabrication process of the optical fiber incorporated with Au NPs in cladding region.

doping solution was prepared by dissolving 0.025 mole of reagent grade $Au(OH)_3$ powder (Aldrich Chem. Co. Inc., 99.9 %) in nitric acid solution (Junsei Co., 70 %). To make a solid glass rod, known as a preform, the porous germano-silicate layers were deposited onto the inner surface of a silica glass tube by using primarily silicon tetrachloride ($SiCl_4$) and germanium tetrachloride ($GeCl_4$) in MCVD process. To incorporate Au NPs, the porous deposition layers were soaked with Au doping solution for two hours and the tube was dried and sintered. Then a silica glass rod (refractive index, n = 1.4571 @ 633 nm) was inserted in the tube and consolidated into a rod to obtain a fiber preform. To reveal the doped layers to surface of the rod as a cladding, the outer part of the glass rod that was the silica glass tube, was etched off using hydrofluoric acid solution (J. T. Baker, 49%). The final preform consisted of the cladding doped with Au NPs in germano-silicate glass and the core of pure silica glass. Finally, the fiber preform was drawn into a fiber with 124.3 μm in diameter using the draw tower at 2150 °C. During the drawing process, the fiber was coated with lower refractive index polymer (EFIRON UVF PC-375, n = 1.3820) than that of the germano-silicate glass of the cladding to induce total internal reflection for light transmission. A process flow steps to fabricate the optical fiber incorporated with Au NPs in cladding region are shown in Figure 1.

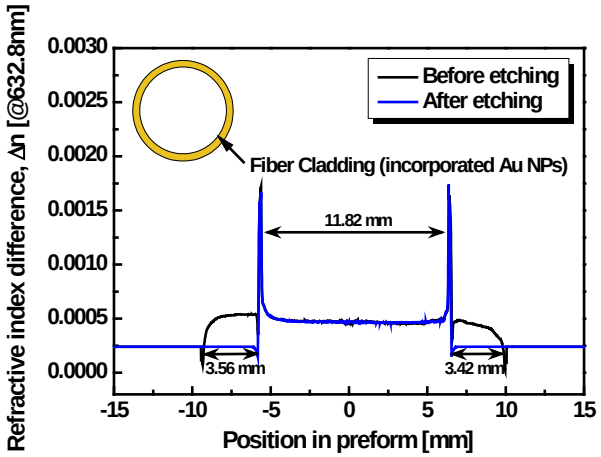

Figure 2. Measured refractive index profile of the fiber preform incorporated with Au NPs in cladding region (Inset: cross-section of the preform).

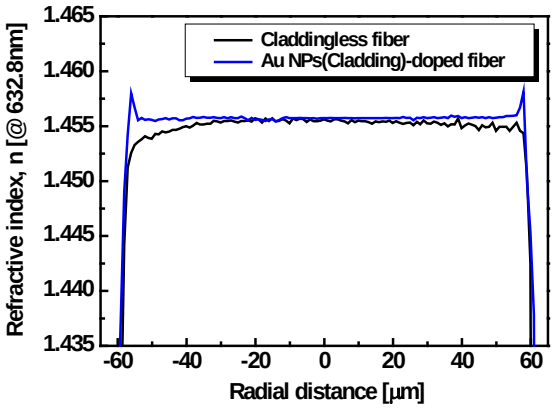

Figure 3. Measured refractive index profile of the optical fiber incorporated with Au NPs in cladding region.

Figure 2 and Figure 3 show the measured refractive index profile of the fabricated optical fiber preform before and after the etching process and the optical fiber incorporated with Au NPs in cladding region, respectively. Successful removal of the silica glass tube by the etching process was indicated by the measured indices of the preform and the fiber as shown in Figure 2 and Figure 3, respectively. The refractive index difference between the core and cladding was about 0.00125, enabling light signal to propagate into the cladding region not into the core, as shown in Figure 4. The cladding width and total diameter of the optical fiber were 2.6 μm and 124.3 μm, respectively. To confirm formation of Au NPs in the cladding, the optical fiber preforms were examined by transmission electron microscope (TEM, FEI Tecnai G2 F30 S-TWIN) and UV-VIS spectrophotometer (Varian, Cary500Scan). Optical absorption of the optical fibers was also measured to confirm the propagation of light and the existence of Au NPs by the cut-back method using the Optical Spectrum Analyzer (Ando AQ 6315B). Then, to characterize SPR sensing property, optical absorption of the fiber was measured by putting small drops of the refractive index matching oil with various refractive indices (n = 1.406 - 1.436) on the surface of the fiber. The total and detector length of the fiber used for the SPR measurement are 50 cm and 5 cm, respectively, as shown in Figure 5.

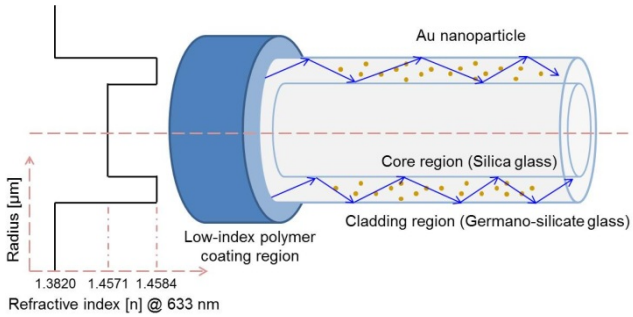

Figure 4. Refractive index and the propagation of light through the cladding of the fiber doped with Au NPs.

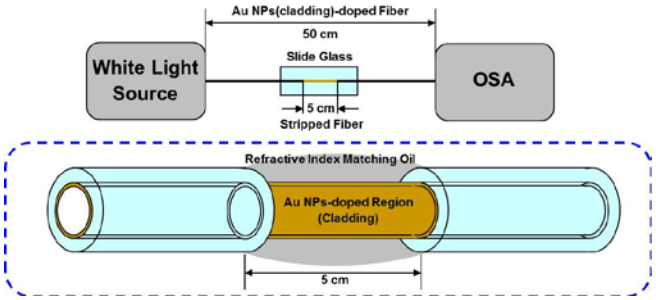

Figure 5. Schematic of the SPR measurement set-up using the optical fiber incorporated with Au NPs in cladding region.

III. RESULTS AND DISCUSSION

Figure 6 compares the UV-VIS spectra of the optical fiber preform incorporated with and without Au NPs. The absorption band centering at 585 nm was found to appear after the incorporation of Au NPs and it was attributed to Au NPs in the cladding region of the preform [29-31]. The existence and size distribution of Au NPs of the preform was verified by the TEM morphology of the fiber preform, as shown in Figure 7. The Au NPs was found to be crystalline and the rather spherical particles were dispersed homogeneously without agglomeration. The average

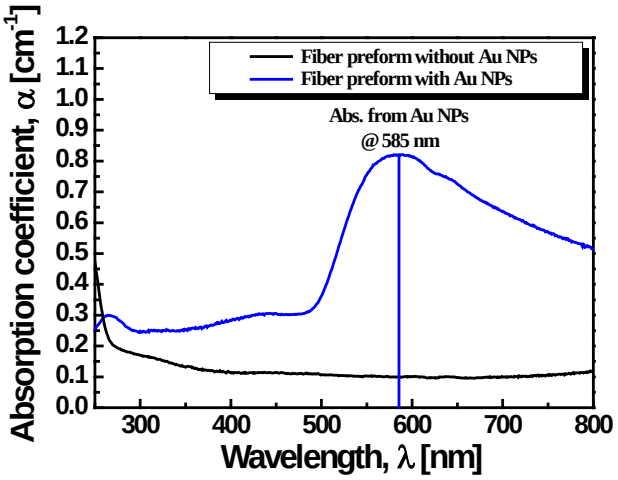

Figure 6. UV-VIS spectra of the optical fiber preform incorporated with and without Au NPs in cladding region.

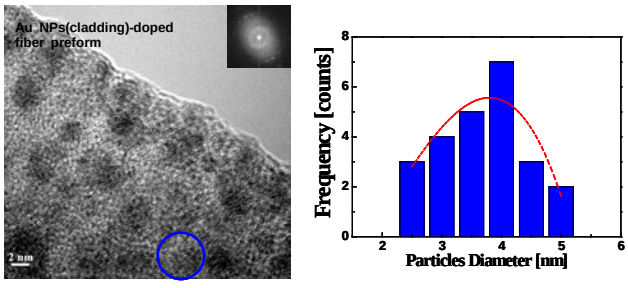

Figure 7. TEM image and the size distribution of Au NPs incorporated in the cladding of the optical fiber preform.

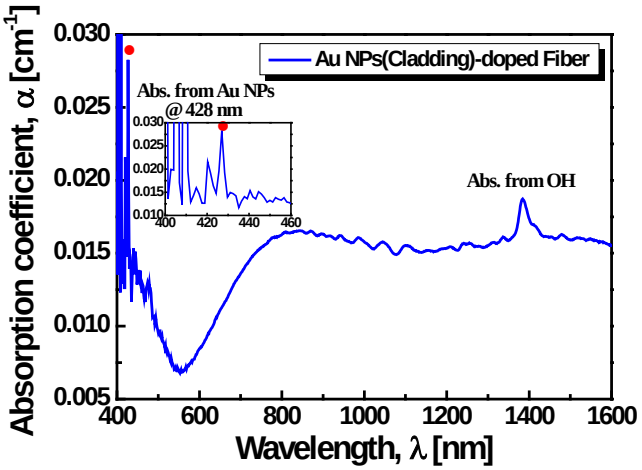

Figure 8. Absorption spectrum of the optical fiber incorporated with Au NPs in cladding region.

diameter of Au NPs was ~ 3.8 nm (2.5 nm ~ 5.2 nm). Note that peak position of the optical absorption is known to depend on the particle size of Au metals [31-33].

In the case of optical fiber, which was drawn from the fiber preform incorporated with Au NPs, the existence of Au NPs was verified by optical absorption spectra, as shown in Figure 8. Absorption peaks appeared at 428 nm and 1380 nm and they are due to surface plasmon resonance from Au NPs and OH impurities, respectively [30-34]. Note that to extract the absorption peak from the detector noise, we performed the spectral decomposition and denoising by using the OriginPro-8.6 code, which clearly distinguishes the absorption peak at 428 nm as shown in Figure 9.

As per earlier reported work, the Au NP related absorption peak has been observed at around 520 nm; however we measured the absorption peak at 585 nm in the optical fiber preform. Moreover, the absorption peak due to Au NPs was found to shift to shorter wavelength of 428 nm in the optical fiber as compared to 585 nm peak in the

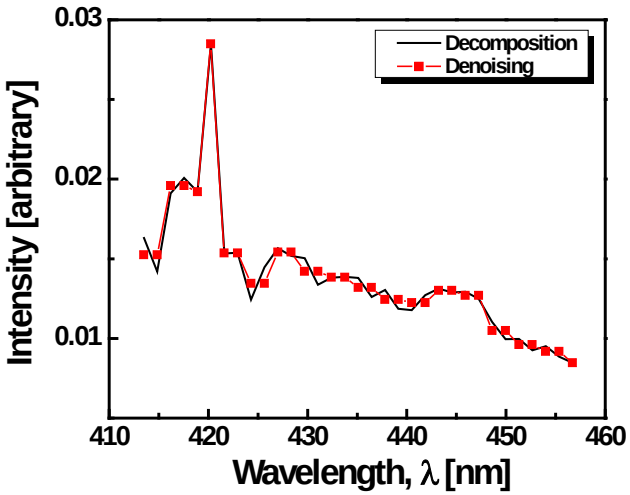

Figure 9. Resolving the absorption peak in the optical fiber incorporated with Au NPs in cladding region.

 ISBN: 978-1-61208-208-0

preform. As we needed to heat the fiber preform at 2150 °C to draw the fiber, Au NPs size would increase due to the growth of Au NPs after the high temperature drawing process. Thus, our sample showed the blue-shift of Mie resonance absorption peak with increment in the size of nano-particles, which is quite opposite behavior where increment in nano-particles size gives red shift in the absorption peak [35-37].

The blue-shift of SPR peak with the increase of nano-particles size is not a new behavior, it has been already reported for Au particles in Au-alumina composite film [38] and Au NPs dispersed within pores of porous silica [31-33]. The peak position from Mie resonance is almost independent of the size of Au particles in the range from 4 to 25 nm (by using the dielectric constant of Au [31][39][40]. The blue-shift can be thought to be due to association with the boundary coupling (interface interaction) between Au particles within the pores and pore walls of porous silica [31]. Usually, a small lattice contraction yields to the high surface-to-volume ratio and, hence, high surface energy (surface tension) for metal NPs. The lattice dilatation in [31-33], it is probably related to the decreased surface energy of Au particles via boundary coupling. It is well known that at the surface of small particles, there exist many dangling bonds (unsaturated bonds). In other words, the extension of electronic wave function outside particles surface becomes significant for small particles. Thus, interactions at the particles' surface are inevitable due to the high activity, and charge transfer from metal particles to the matrices occurs during interface interaction. This charge transfer can induce a decrease of the free electron density in metal particles. Therefore, the blue-shift occurs with the increase of Au particle size due to the electron charge transfer from Au particles to the silicate glass host at the interface.

Figure 10 shows the absorption spectra of the optical fiber after dropping the index matching oils (n = 1.406 - 1.436) to confirm the SPR and its dependence of environmental change. Because of noisy behavior of the output spectrum, FFT (Fast Fourier Transform) filtering method was adopted to locate peaks. The SPR band was found to occur at a particular wavelength around 500 nm for the corresponding refractive indices, increased with the increase of the index [1, 3][8-11]. The measured peak wavelength of the SPR band were at 480.9 nm, 483.3 nm, 494.4 nm, and 505.5 nm with refractive indices (n) 1.406, 1.416, 1.426, and 1.436, respectively as shown in Figure 11. The observed red-shift of the SPR band with the increase of the refractive index of matching oils is related to the angle of incident light, increased with the increase of refractive index [1-3][8-11]. The shift of the Au plasmon peak towards a longer wavelength with the increase of the medium refractive index can be understood by the well-known Mie theory. It is noted that the absorption peak of the fiber coated with low-index polymer (n=1.382) appearing at 428 nm due to surface plasmon resonance from Au NPs was also found to shift to ~ 500 nm after dropping the index matching oils, which is basically an extension phenomenon by the Mie theory. The SPR sensitivity (wavelength/RIU), which is the slope of Figure 11, of the optical fiber incorporated with Au

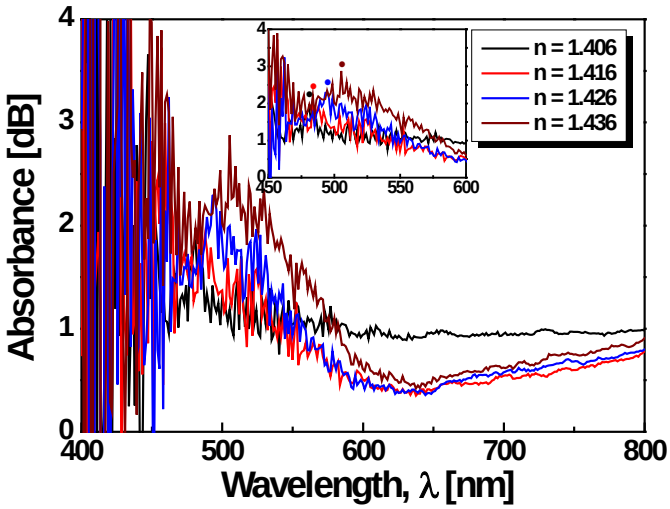

Figure 10. Absorption spectra of the Au NPs(cladding)-doped optical fiber covered with the index matching oils of different refractive indices (n = 1.406 - 1.436).

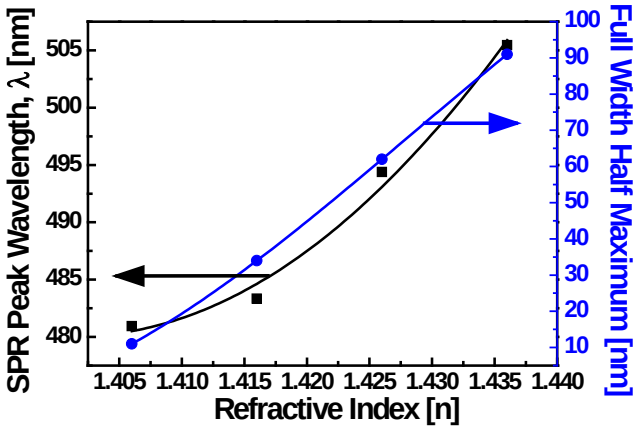

Figure 11. Peak and width change of the surface plasmon resonance (SPR) peak of the Au NPs(cladding)-doped optical fiber covered with the index matching oils of different refractive indices (n = 1.406-1.436).

NPs was estimated to be 820 nm/RIU. Indeed, the SPR sensitivity of optical fiber sensor based on glass optical fiber incorporated with Au NPs in the cladding region is smaller than that of the conventional Au thin film based optical fiber SPR sensor, which has about 9,630 nm/RIU [41]. However, 820 nm/RIU is still a valuable level to identify the possibility of a new type fiber SPR sensor for its advantage of mass production. In this paper, we have focused on the fabrication of specialty optical fiber incorporated with Au NPs in cladding region for SPR sensor applications, which is the first in the world to the best of our knowledge. Increase of the sensitivity of the sensor is under progress and will be communicated in future.

It is noted that the increase in intensity and width of the SPR absorption band was also found to be 1.5 dB and 91 nm (after baseline correction), respectively with the increase of the refractive index from 1.406 to 1.436. The broadening of the SPR absorption may be due to the spatial spreading and scattering of the conduction electrons [42].

 ISBN: 978-1-61208-208-0

The proposed fiber sensor based on optical fiber incorporated with Au NPs in the cladding region has the clear advantages over the conventional Au thin film based optical fiber SPR sensor such that the bulk metal film coating is not necessary after post-processings of fiber polishing and tapering to satisfy the phase matching criterion for excitation. Since no metal coating is needed for the sensor, mass production with simple fiber fabrication is possible and compatibility with the existing SPR probe is secured.

IV. CONCLUSION

We developed and demonstrated specialty optical fiber incorporated with Au NPs in cladding region for SPR sensor applications. The optical fiber incorporated with Au NPs in cladding region was fabricated by using the modified chemical vapor deposition (MCVD) and the fiber drawing process. Porous germano-silicate layers were deposited onto the inner surface of a silica glass tube and the layers were soaked with Au doping solution to incorporate Au NPs followed by drying and sintering. Then a silica glass rod (refractive index, n = 1.4571 @ 633 nm) was inserted in the tube and consolidated into a rod and the outer silica glass was etched off to obtain a fiber preform incorporated with Au NPs in cladding region. Finally, the fiber preform was drawn and coated with the lower refractive index polymer (EFIRON UVF PC-375, n = 1.3820) than that of the cladding to obtain a fiber with the cladding width of 2.6 μm and total diameter of 124.3 μm.

The measured SPR absorption band centered at 585 nm of the optical fiber preform was attributed to the large concentration of the Au NPs with the average diameter of 3.8 nm. In the case of the fiber, the SPR absorption peak due to Au NPs was found to shift to 428 nm as compared to 585 nm of the preform. This blue-shift is due to the increase of the particle size through the growth of the Au NPs during the fiber drawing process at 2150 °C, the absorption band of Au NPs within pores of porous silica yielded the significant blue-shift, which was interpreted in terms of interface interactions between Au NPs and silica glass host. The blue-shift of the absorption band in the present study may originate from the electron transfer from Au particles to the silica host during interfacial interaction.

The SPR absorption peak due to Au NPs in the bare optical fiber was found to appear at 428 nm. When the index matching oils was dropped onto the fiber, the SPR was found to occur at a particular wavelength around 500 nm. The measured peak wavelength of the SPR increased from 480.9 nm to 505.5 nm with refractive index (n) from 1.406 to 1.436. The SPR sensitivities of the optical fiber incorporated with Au NPs in cladding region was estimated to be 820 nm/RIU.

ACKNOWLEDGMENTS

This work was supported partially by the Ministry of Science and Technology, the NRF through the research programs (No. 2008-0061843 and No. 20100020794), the New Growth Engine Industry Project of the Ministry of Knowledge Economy, the Core Technology Development Program for Next-generation Solar Cells of Research Institute of Solar and Sustainable Energies (RISE), the Brain Korea-21 Information Technology Project, and by the (Photonics2020) research project through a grant provided by the Gwangju Institute of Science and Technology in 2012, South Korea.

REFERENCES

[1] J. Homola, S. S. Yee, and G. Gauglitz, “Surface plasmon resonance sensors: review,” Sens. Actuators B, vol. 54, pp. 3-15, September 1999.

[2] C. van Trigt, “Visual system-response functions and estimating reflectance,” JOSA A, vol.14, pp. 741-755, April 1997.

[3] A. K. Sharma, R. Jha, and B. D. Gupta, “Fiber-optic sensors based on surface plasmon resonance: A comprehensive review,” IEEE Sens. J., vol. 7, pp. 1118-1129, August 2007.

[4] B. D. Gupta and R. K. Verma, “Review article: Surface plasmon resonance-based fiber optic sensors: Principle, probe designs, and some applications,” J. Sens., vol. 2009, pp. 1-12, June 2009.

[5] C. R. Yonzon, E. Jeoung, S. Zou, G. C. Schatz, M. Mrksich, and R. P. V. Duyne, “A comparative analysis of localized and propagating surface plasmon resonance sensors: The binding of concanavalin A to a monosaccharide functionalized self-assembled monolayer,” J. Am. Chem. Soc., vol. 126, pp. 12669-12676, September 2004.

[6] S. Singh and B. D. Gupta, “Simulation of a surface plasmon resonance-based fiber-optic sensor for gas sensing in visible range using films of nanocomposites,” Meas. Sci. Technol., vol. 21, pp. 115202, September 2010.

[7] A. K. Sharma and B. D. Gupta, “Simulation of a localized surface-plasmon-resonance-based fiber optic temperature sensor,” Opt. Soc. Am., vol. A 27, pp. 1743-1749, July 2010.

[8] Y. Lin, Y. Zou, and R. G. Lindquist, “A reflection-based localized surface plasmon resonance fiber-optic probe for biochemical sensing,” Biomed. Opt. Express, vol. 2, pp. 478-484, March 2011.

[9] A. S. Yeri, L. Gao, and D. Gao, “Mutation screening based on the mechanical properties of DNA molecules tethered to a solid surface,” J. Phys. Chem. B, vol. 114, pp. 1064-1068, January 2010.

[10] R. Slavík, J. Homola, J. Čtyroký, and E. Brynda, “Novel spectral fiber optic sensor based on surface plasmon resonance,” Sens. Actuators B, vol. 74, pp. 106–111, April 2001.

[11] M. Mitsushio, S. Higashi, and M. Higo, “Construction and evaluation of a gold-deposited optical fiber sensor system for measurements of refractive indices of alcohols,” Sens. Actuators A, vol. 111, pp. 252–259, March 2004.

[12] B. Liedberg, C. Nylander, and I. Lunström, “Surface plasmon resonance for gas detection and biosensing,” Sens. Actuators, vol. 4, pp. 299-304, May-June 1983.

[13] H. Reather, Surface plasmons on smooth and rough surfaces and on gratings (Springer-Verlag: Berlin, 1988).

[14] F. Yu, S. Ahl, A.-M. Caminade, J.-P, Majoral, W. Knoll, and J. Erlebacher, “Simultaneous excitation of propagating and localized surface plasmon resonance in nanoporous gold membranes,” Anal. Chem., vol. 78, pp. 7346-7350, October 2006.

[15] T. R. Jensen, G. C. Schatz, and R. P. Van Duyne, “Nanosphere lithography: Surface plasmon resonance spectrum of a periodic array of silver nanoparticles by

 ISBN: 978-1-61208-208-0

ultraviolet-visible extinction spectroscopy and electrodynamic modeling," J. Phys. Chem. B, vol. 103, pp. 2394-2401, February 1999.

[16] J. M. Steele, Z. Liu, Y. Wang, and X. Zhang, "Resonant and non-resonant generation and focusing of surface plasmons with circular gratings," Opt. Express, vol. 14, pp. 5664-5670, June 2006.

[17] N. Nath and A. Chilkoti, "Label-free biosensing by surface plasmon resonance of nanoparticles on glass: Optimization of nanoparticle size," Anal. Chem., vol. 76, pp. 5370-5378, August 2004.

[18] S. H. Chang, S. K. Gray, and G. C. Schatz, "Surface plasmon generation and light transmission by isolated nanoholes and arrays of nanoholes in thin metal films," Opt. Express, vol. 13, pp. 3150-3165, April 2005.

[19] J. Aizpurua, P. Hanarp, D. S. Sutherland, M. Kall, G. W. Bryant, and F. J. G. de Abajo, "Optical properties of gold nanorings," Phys. Rev. Lett. , vol. 90, pp. 057401, February 2003.

[20] J. Fu, B. Park, and Y. Zhao, "Nanorod-mediated surface plasmon resonance sensor based on effective medium theory," App. Opt., vol. 48, pp. 4637-4649, August 2009.

[21] J. Kim, G. L. Liu, Y. Lu and L. P. Lee, "Spectral tuning of localised surface plasmon-polariton resonance in metallic nano-crescents," IEE Proc.-Nanobiotechnol., vol. 153, pp. 42-46, June 2006.

[22] Z. W. Liu, Q. H. Wei, and X. Zhang, "Surface plasmon interference nanolithography," Nano. Lett., vol. 5, pp. 957-961, April 2005.

[23] N. Halas, "Playing with plasmons. Tuning the optical resonant properties of metallic nanoshells," MRS Bull., vol. 30, pp. 362-367, May 2005.

[24] P.-Y. Chung, T.-H. Lin, G. Schultz, C. Batich, and P. Jiang, "Nanopyramid surface plasmon resonance sensors," Appl. Phys. Lett., vol. 96, pp. 261108, July 2010.

[25] L. S. Live, O. R. Bolduc, and J.-F. Masson, "Propagating surface plasmon resonance on microhole arrays," Anal. Chem., vol. 82, pp. 3780-3787, March 2010.

[26] G. P. Anderson, J. P. Golden, L. K. Cao, D. Wijesuriya, L. C. Shriver-Lake, and F. S. Ligler, "Development of an evanescent wave fiber optic biosensor," IEEE Eng. Med. Biol. Mag., vol. 13, pp. 358-363, June-July 1994.

[27] T.-C. Peng, W.-C. Lin, C.-W. Chen, D. P. Tsai, and H.-P. Chiang, "Enhanced sensitivity of surface plasmon resonance phase-interrogation biosensor by using silver nanoparticles," Plasmonics, vol. 6, pp. 29-34, September 2011.

[28] K.-S. Lee and M. A. El-Sayed, "Gold and silver nanoparticles in sensing and imaging: sensitivity of plasmon response to size, shape, and metal composition," J. Phys. Chem. B, vol. 110, pp. 19220-19225, September 2006.

[29] J. Matsuoka, R. Mizutani, S. Kaneko, H. Nasu, K. Kamiya, K. Kadono, T. Sakaguchi, and M. Miya, "Sol-Gel processing and optical nonlinearity of gold colloid-doped silica glass," J. Ceram. Soc. Jpn., vol. 101, pp. 53-58, January 1993.

[30] S. Ju, N. V. Linh, P. R. Watekar, B. H. Kim, C. Jeong, S. Boo, C. J. Kim, and W.-T. Han, "Fabrication and optical characteristics of a novel optical fiber doped with the Au nano-particles," J. Nanosci. Nanotechnol., vol. 6, pp. 3555-3558, November 2006.

[31] H. Shi, L. Zhang, and W. Cai, "Preparation and optical absorption of gold nanoparticles within pores of mesoporous silica," Mater. Res. Bull., vol. 35, pp. 1689-1691, December 2000.

[32] W. Cai, H. Hofmeister, T. Rainer, and W. Chen, "Optical properties of Ag and Au nanoparticles dispersed within the pores of monolithic mesoporous silica," J. Nanopart. Res., vol. 3, pp. 443-453, June 2001.

[33] A. E. Badger, W. Weyl, and H. Rudow, "Effect of heat-treatment on color of gold-ruby glass," Glass Ind., vol. 20, pp. 407-414, November 1939.

[34] J. Stone, "Reduction of OH absorption in optical fibers by OH → OD isotope exchange," Ind. Eng. Chem. Prod. Res. Dev., vol. 25, pp. 609-621, December 1986.

[35] S. Link and M. A. El-Sayed, "Spectral properties and relaxation dynamics of surface plasmon electronic oscillations in gold and silver nanodots and nanorods," J. Phys. Chem., vol. 103, pp. 8410-8426, September 1999.

[36] M.-C. Daniel and D. Astruc, "Gold nanoparticles: assembly, supramolecular chemistry, quantum-size-related properties, and applications toward biology, catalysis, and nanotechnology," Chem. Rev., vol. 104, pp. 293-346, January 2004.

[37] S. J. Oldenburg, R. D. Averitt, S. L. Westcott, and N. J. Halas, "Nanoengineering of optical resonances," Chem. Phys. Lett., vol. 288, pp. 243-247, March 1998.

[38] Y. Hosoya, T. Suga, T. Yanagawa, and Y. Kurokawa, "Linear and nonlinear optical properties of sol-gel-derived Au nanometer-particle-doped alumina" J. Appl. Phys., vol. 81, pp. 1475-1480, October 1997.

[39] C. F. Bohren and D. R. Huffman, Absorption and scattering of light by small particles; Chapter. 12 (John Wiley & Sons, New York, 1983.

[40] M. Otter, "Optische konstanten massiver metalle," Z. Physik, vol. 161, pp. 163-178, April 1961.

[41] S. Ju, S. Jeong, Y. Kim, P. Jeon, H. S. Kim, M.-S. Park, J.-H. Jang, and W.-T. Han "Surface Plasmon Resonance of Au/Ti Coated Tapered Optical Fiber," in Proceedings of The 5th International Conference on Surface Plasmon Photonics, (Academic, Busan, Korea, 2011), TUP-72, May 2011.

[42] Y. Zhang, A. H. Yuwono, J. Li, and J. Wang, "Highly dispersed gold nanoparticles assembled in mesoporous titania films of cubic configuration," Micropor. Mesopor. Mater., vol. 110, pp. 242–249, June 2007.

 ISBN: 978-1-61208-208-0